Rare Metal Materials and Engineering
Volume 53, Issue 9, September 2024
Available online at www.rmme.ac.cn

Science Press

Cite this article as: Zang Ximin, Zhao Guangdi, Wu Jinjiang, et al. Influence of Holding Time on Hot Deformation Behavior of Hard-Deformed Superalloy U720Li[J]. Rare Metal Materials and Engineering, 2024, 53(09): 2446-2457. DOI: 10.12442/j.issn.1002-185X.20230790.

ARTICLE

Influence of Holding Time on Hot Deformation Behavior of Hard-Deformed Superalloy U720Li

Zang Ximin[1], Zhao Guangdi[2], Wu Jinjiang[2], Jiang Haoyuan[2], Yao Xiaoyu[3]

[1] School of Materials Science and Engineering, Shenyang University of Technology, Shenyang 110870, China; [2] School of Materials and Metallurgy, University of Science and Technology Liaoning, Anshan 114051, China; [3] Institute of Metal Research, Chinese Academy of Sciences, Shenyang 110016, China

Abstract: To improve the hot workability of hard-deformed superalloy U720Li, the effect of holding time before deformation (5 and 10 min) on hot deformation behavior was investigated by hot compression tests. Results show that the flow stress increases with increase in strain rate, while decreases with increase in deformation temperature and holding time. Based on the obtained Arrhenius-type constitutive models, the calculated peak stresses are in good agreement with experimental values, indicating that this model can accurately predict the hot deformation behavior of U720Li alloy, and the deformation activation energies for the holding time of 5 and 10 min were calculated to be 992.006 and 850.996 kJ·mol^{-1}, respectively. Moreover, processing maps of U720Li alloy with these two holding durations were constructed. Through observation of deformation microstructures in each domain of the processing maps, the optimal hot working conditions for the holding time of 5 min are determined to be 1090–1110 °C/ 1–10 s^{-1} and 1146–1180 °C/1–10 s^{-1}, and the optimal hot working conditions for the holding time of 10 min are 1080–1090 °C/1–10 s^{-1} and 1153–1160 °C/1–10 s^{-1}, indicating that the safe processing window can be obviously enlarged by shortening the holding time reasonably. In the absence of cracking, the dynamic recrystallization (DRX) grain size increases gradually with increasing the deformation temperature and holding time, but it first decreases and then increases with the increase in strain rate. When the deformation temperature is below 1100 °C, the DRX mechanism is mainly the particle-induced continuous DRX. As the temperature is raised to above 1130 °C, the main DRX mechanism changes to discontinuous DRX.

Key words: hard-deformed superalloy; hot deformation behavior; processing map; dynamic recrystallization

Ni-based superalloys are key materials for manufacturing aeroengine turbine discs because of their excellent high temperature strength, creep resistance and fatigue resistance[1–2]. Forging is the most widely used forming method to prepare turbine discs. During the forging process, the deformation behavior and microstructure of Ni-based superalloys are very sensitive to the process parameters, such as temperature, strain rate and strain[3]. U720Li is a typical hard-deformed Ni-based superalloy with extremely high alloying degree. The volume fraction of strengthening phase γ' reaches about 50vol% and the solvus temperature of γ' is as high as 1160 °C, which seriously deteriorates its hot workability[4]. Until now, how to expand the hot working window of such hard-deformed superalloys is still a challenge.

Constitutive models and processing maps are critical to characterize the flow stress behavior, optimize process parameters and control the microstructure evolution of superalloys during hot deformation[5]. There are currently several studies on the hot deformation behavior of U720Li alloy. Qu et al[6] established the constitutive equation and processing map, and found that dynamic recrystallization (DRX) is the dominant softening mechanism during hot deformation. Li et al[7] proposed that the DRX can be promoted by raising the deformation temperature and lowering the strain rates. Yu et al[8] constructed the processing maps and discussed the instability mechanism. Recently, Wan et al[9] identified optimum hot deformation conditions for the γ/γ' dual-phase range and quasi-γ phase range based on the processing map and deformation microstructures.

It is well accepted that the microstructure evolution of

Received date: December 05, 2023
Foundation item: National Natural Science Foundation of China (52174317, 51904146)
Corresponding author: Zhao Guangdi, Ph. D., Associate Professor, School of Materials and Metallurgy, University of Science and Technology Liaoning, Anshan 114051, P. R. China, Tel: 0086-412-5929381, E-mail: gdzhao12s@alum.imr.ac.cn

superalloys during forging process is mainly due to the occurrence of DRX[10]. However, the DRX mechanism of U720Li alloy remains controversial at present. For example, Li et al[11] found that the DRX mechanism in γ/γ' dual phase range is the quasi-continuous dynamic recrystallization (quasi-CDRX) plus discontinuous dynamic recrystallization (DDRX), but that in γ single-phase range is mainly DDRX. Wan[12] found that the DRX mechanism is particle induced-continuous dynamic recrystallization (PI-CDRX) plus DDRX at low temperatures (1060–1120 °C), and mainly DDRX at high temperatures (1140–1180 °C).

In the actual forging process, superalloy billets are always heated for a definite time before deformation. Our recent study has found that the holding time has a significant influence on the volume fraction and size of γ' phase[13]. Extensive literature research suggests that the flow stress behavior and DRX mechanism of Ni-based superalloys are closely related to γ' characteristics[10,14–15]. Hence, the holding time before deformation can cause significant influence on the hot workability and microstructure of U720Li alloy, which in turn affects the mechanical properties of forgings. However, the existing relevant research is mainly focused on the effects of deformation temperature, strain rate and strain[3,16–17]. To the best of our knowledge, there are few reports on how the holding time affects the hot workability of U720Li alloy.

Therefore, the influence of holding time on the hot deformation behavior and DRX mechanism of U720Li alloy was investigated in this research. Arrhenius-type constitutive models and processing maps for two holding durations were established, and the optimum deformation conditions were determined according to the microstructure observation of each processing domain. The results can provide theoretical guidance for optimizing the forging process of U720Li alloy and improving mechanical properties of the forgings.

1 Experiment

1.1 Materials

The U720Li alloy bar with 110 mm in diameter provided by the Western Superconducting Material Technologies Co., Ltd was used as the experimental material. The alloy bar was prepared by hot forging after triple melting process (vacuum induction melting+electroslag remelting+vacuum arc remelting). Its chemical composition was determined by the iCAP6300 inductively coupled plasma-atomic emission spectrometry (ICP-AES), and the result is listed in Table 1.

Specimens with a dimension of 10 mm×10 mm×10 mm were cut from half radius of the bar through a wire-electric discharge machine. Then, they were polished and chemically etched in a solution of 10 g $CuCl_2$+100 mL HCl+100 mL C_2H_5OH for about 10 min. The original microstructure of U720Li alloy bar was observed by Axio Vert. A1 optical microscope (OM), as shown in Fig. 1. It can be seen that the initial grain structure is quite uniform and equiaxed, and there are lots of γ' particles with the morphology more or less spherical distributed along the grain boundaries. The quantitative measurement result by Nano-Measurer 1.2 software indicates that the average size of initial grains is about 23 μm.

Table 1 Chemical composition of U720Li alloy bar (wt%)

B	C	Al	Ti	Cr	Co	W	Zr	Mo	Ni
0.014	0.021	2.41	5.11	15.78	14.5	1.20	0.043	2.92	Bal.

1.2 Hot compression test

Hot compression tests were performed on the thermal simulation machine (THERMECMASTOR, 100 kN) under vacuum to study the hot deformation behavior of U720Li alloy in different process conditions. Cylindrical specimens with the dimension of Φ8 mm×12 mm for the tests were cut from half radius of the bar. The deformation temperature was 1050–1180 °C, the strain rate was 0.01–10 s^{-1}, and all tests were conducted to a true strain of 0.8. The specimens were heated at a heating rate of 10 °C·s^{-1} to the deformation temperature, and held for 5 and 10 min before deformation. The selection of these two holding time is mainly because the γ' characteristic and grain size of U720Li alloy after holding at a certain temperature for 5 and 10 min are different obviously. Moreover, the overlong holding time will lead to a very coarse grain structure, which is harmful to the hot workability and mechanical properties of the alloy[13]. After compression, the specimens were immediately cooled by ejecting argon, and hence the deformation microstructure was preserved. Fig. 2 presents the schematic depiction of the compression tests. In

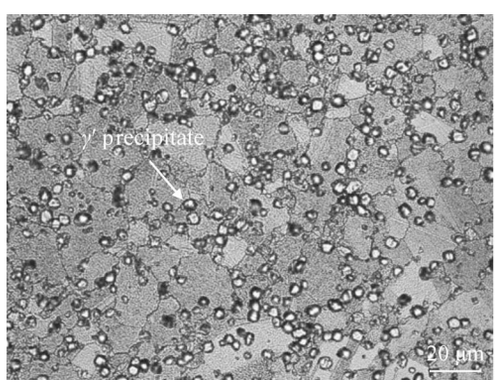

Fig.1 Original microstructure of U720Li alloy bar

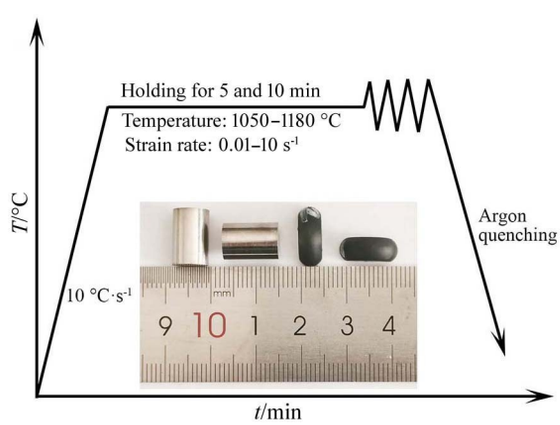

Fig.2 Schematic diagram of the hot compression tests

order to minimize the friction between specimens and dies, mica plates were placed between them. Besides, a K-type thermocouple was applied to control the temperature.

Afterwards, the compressed specimens were sliced parallel to the compression axis through the center. The sliced surfaces were ground and polished, and then etched by the above method. The deformation microstructures were observed by OM. The average DRX grain size was measured by the Nano-Measurer 1.2 software. To ensure the measurement reliability, five optical micrographs (×500) were taken for each specimen to calculate the average value.

2 Results and Discussion

2.1 True stress-true strain curves

Fig. 3 shows the true stress-true strain curves of U720Li alloy at different strain rates and deformation temperatures with a holding time of 5 min. The flow stress curves under different test conditions exhibit similar characteristics. In the early deformation stage, the flow stress increases rapidly to the peak stress, which is mainly owing to the work hardening caused by dislocation generation and multiplication[18]. Since the stacking fault energy of U720Li alloy is low, the increase in dislocation density will lead to the occurrence of DRX once the deformation degree exceeds the critical strain. As the deformation degree increases, the DRX becomes the main softening mechanism, causing the decrease in flow stress. When the work hardening and dynamic softening reach a dynamic equilibrium, the flow stress maintains at a steady value with increasing the strain. In addition, the flow stress decreases with increasing the deformation temperature or decreasing the strain rate. This may be because higher temperatures accelerate the dissolution of γ', which weakens its pinning effect on migration of dislocations and grain boundaries[15]; the lower strain rate favors the growth of DRX nuclei for the sufficient time, and decreases the dislocation proliferation rate[12].

It is worth noting that the flow stress curves of the alloy deformed at temperatures higher than 1100 °C and strain rates greater than 0.1 s^{-1} exhibit a yield drop phenomenon, and the yield drop magnitude increases markedly with the increase in strain rate. Similar phenomenon was also observed for other Ni-based superalloys such as IN100, WASPALOY and U720[15,19]. Guimaraes et al[20] proposed that the occurrence of yield drop for WASPALOY alloy above the γ' solvus temperature is due to the short-range ordered locking of dislocations. Monajati et al[15] suggested that the higher temperature leads to higher γ' dissolution degree, which results in the release of more Al and Ti atoms from the γ'. Then, a larger number of Al and Ti atoms act as solutes in the matrix, which strongly impedes the movement of dislocations and ultimately locks them. The greater yield drop magnitude at higher strain rates should be mainly attributed to the higher dislocation density, which causes more interactions between dislocations and solutes[15]. Besides, for the flow stress curves at the deformation temperature of 1050 °C and strain rates lower than 1 s^{-1}, abnormal increase in the flow stress occurs as the true strain reaches around 0.6 (Fig.3a–3c). This is because the deformation under such conditions is uneven, which leads to over-spread of compressed specimens at larger strains and hence increases the friction[21].

Fig. 4 shows the true stress-true strain curves of U720Li alloy at different strain rates and deformation temperatures with a holding time of 10 min before deformation. The flow stress curves have similar characteristics with the flow stress

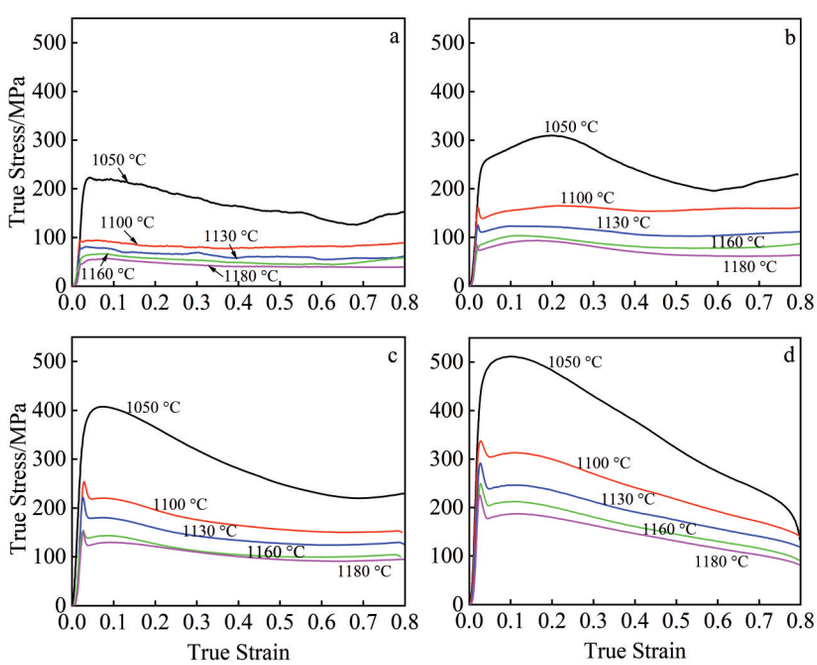

Fig.3 True stress-true strain curves of U720Li alloy with a holding time of 5 min before deformation: (a) 0.01 s^{-1}, (b) 0.1 s^{-1}, (c) 1 s^{-1}, and (d) 10 s^{-1}

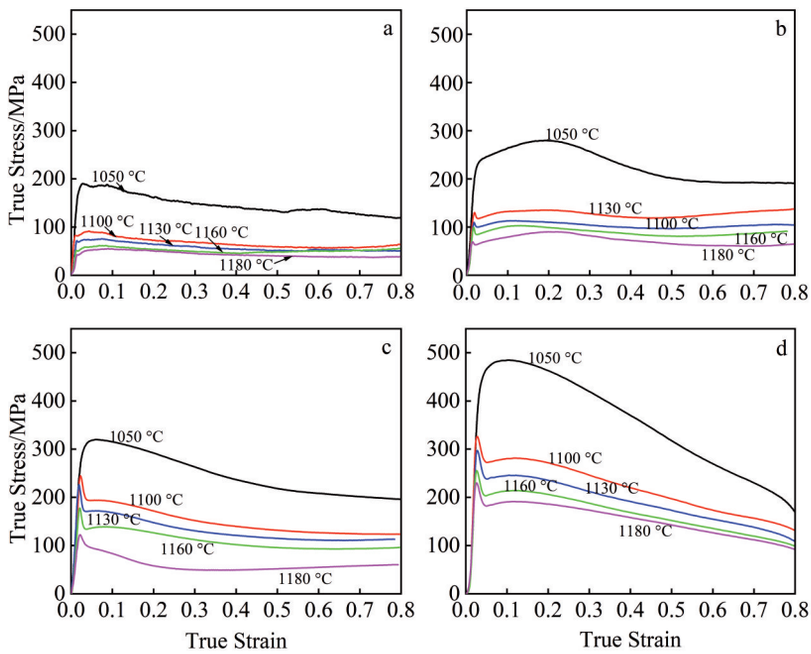

Fig.4 True stress-true strain curves of U720Li alloy with a holding time of 10 min before deformation: (a) 0.01 s^{-1}, (b) 0.1 s^{-1}, (c) 1 s^{-1}, and (d) 10 s^{-1}

curves in Fig.3. However, the flow stress for the holding time of 10 min is significantly lower than that for the holding time of 5 min. Our previous study has found that the volume fraction and size of γ' gradually decrease as the holding time prolongs, which weakens the pinning effect on grain boundaries and results in increase in initial grain size before deformation[13]. Based on the Hall-Petch relationship, increase in initial grain size can decrease the deformation resistance[22]. Besides, the dissolution of γ' reduces the pile-up of dislocations, which decreases the work hardening rate. Hence, the flow stress is lowered as the holding time is prolonged to 10 min. No abnormal increase in flow stress occurs on the flow stress curves, which means that increasing the holding time to 10 min makes the deformation at low temperatures (about 1050 °C) more uniform.

2.2 Arrhenius-type constitutive models

The Arrhenius-type model has been widely used to establish the constitutive relationship among flow stress, deformation temperature and strain rate for superalloys due to its high accuracy. The Zener-Holloman parameter (Z) representing effects of temperature and strain rate on the flow stress can be expressed as follows[9]:

$$Z=\dot{\varepsilon}\exp\left(\frac{Q}{RT}\right)=\begin{cases}A\left[\sinh\left(\alpha\sigma\right)\right]^{n} & \text{all stress level}\\ A_1\sigma^{n_1} & \text{low stress level}\\ A_2\exp\left(\beta\sigma\right) & \text{high stress level}\end{cases} \quad (1)$$

in which $\dot{\varepsilon}$ is the strain rate (s^{-1}); Q is deformation activation energy ($kJ\cdot mol^{-1}$); T is absolute temperature (K); R is gas constant (8.314 $kJ\cdot mol^{-1}\cdot K^{-1}$); σ is the flow stress (MPa); A, A_1, A_2, β and $\alpha=\beta/n_1$ are the material constant; n is the stress exponent.

The peak stress (σ_p) level was employed to describe the hot deformation behavior. By taking the natural logarithm of Eq.(1), Eq.(2) can be obtained:

$$\ln\dot{\varepsilon}+\frac{Q}{RT}=\begin{cases}\ln A+n\ln\left[\sinh\left(\alpha\sigma\right)\right]\\ \ln A_1+n_1\ln\sigma\\ \ln A_2+\beta\sigma\end{cases} \quad (2)$$

The values of β, n_1, n and Q can be calculated through taking partial differential on both sides of Eq.(2)[23–24]:

$$\beta=\left[\frac{\partial\ln\dot{\varepsilon}}{\partial\sigma_p}\right]_T,\ n_1=\left[\frac{\partial\ln\dot{\varepsilon}}{\partial\ln\sigma_p}\right]_T,\ n=\left\{\frac{\partial\ln\dot{\varepsilon}}{\partial\ln\left[\sinh\left(\alpha\sigma_p\right)\right]}\right\}_T \quad (3)$$

$$Q=R\left\{\frac{\partial\ln\dot{\varepsilon}}{\partial\ln\left[\sinh\left(\alpha\sigma_p\right)\right]}\right\}_T\left\{\frac{\partial\ln\left[\sinh\left(\alpha\sigma_p\right)\right]}{\partial\left(1/T\right)}\right\}_{\dot{\varepsilon}} \quad (4)$$

Fig.5 shows the plots used for calculation of n_1, β, α, n, Q and ln$A$ values for the holding time of 5 min. The β and n_1 values can be evaluated from the average slopes of fitting lines of ln$\dot{\varepsilon}$-σ_p (Fig. 5a) and ln$\dot{\varepsilon}$-lnσ_p (Fig. 5b) plots, respectively. Then, $\alpha=\beta/n_1$ will be obtained. The value of n can also be determined by linear regression (Fig. 5c). The Q value can be derived from slopes of ln[sinh($\alpha\sigma_p$)]-1/T curves at different strain rates (Fig. 5d). By substituting the Q and n values into Eq. (2), the value of ln$A$ can be derived from intercepts of fitting lines of ln[sinh($\alpha\sigma_p$)]-1/T plot. As shown in Fig. 5e, there is a good linear correlation between the ln$Z$ and ln[sinh($\alpha\sigma_p$)].

Table 2 shows the average values of n_1, β, α, n, Q and ln$A$ for the holding time of 5 min. By substituting these parameters into Eq. (1) (for all stress level), the constitutive model for this holding time is established as follows:

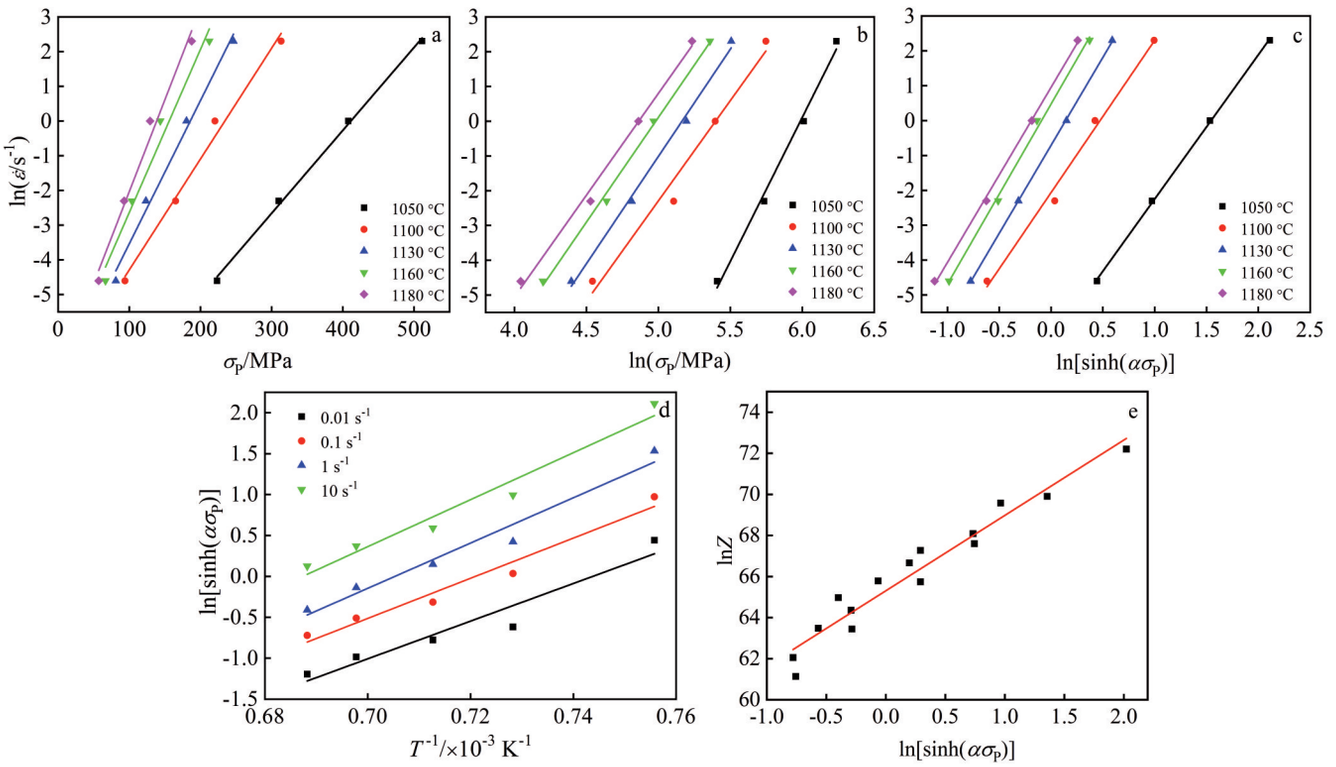

Fig.5 Plots of $\ln\dot{\varepsilon}$-σ_p (a), $\ln\dot{\varepsilon}$-$\ln\sigma_p$ (b), $\ln\dot{\varepsilon}$-$\ln[\sinh(\alpha\sigma_p)]$ (c), $\ln[\sinh(\alpha\sigma_p)]$-$1/T$ (d), and $\ln Z$-$\ln[\sinh(\alpha\sigma_p)]$ (e) for the holding time of 5 min

Table 2 Kinetic parameters of U720Li alloy for the holding time of 5 min

β	n_1	n	α	Q/kJ·mol^{-1}	ln$A$
0.039	6.416	4.618	0.00608	992.006	83.638

$$\dot{\varepsilon}=2.106\times10^{36}\left[\sinh\left(0.00608\sigma_p\right)\right]^{4.618}\exp\left(-\frac{992006}{RT}\right) \quad (5)$$

Fig.6 shows the plots used for calculation of average values of n_1, β, α, n, Q and ln$A$ for the holding time of 10 min. The calculation method for each parameter is the same as that for the holding time of 5 min, and the calculated kinetic parameters are listed in Table 3. It can be seen that the activation energy (Q) for the holding time of 10 min is obviously smaller than that for the holding time of 5 min. This is mainly because the γ' dissolution degree and initial grain size increase with prolonging the holding time, which lowers the deformation resistance of the alloy. However, the activation energies for U720Li alloy with both holding time of 5 and 10 min in this study are markedly higher than those obtained in Ref.[9], which is mainly attributed to the addition of grain boundary strengthening element boron in this study.

Similarly, by substituting the parameters in Table 3 into Eq. (1) (for all stress level), the constitutive model for the holding time of 10 min is established as follows:

$$\dot{\varepsilon}=1.323\times10^{31}\left[\sinh\left(0.00615\sigma_p\right)\right]^{4.569}\exp\left(-\frac{850996}{RT}\right) \quad (6)$$

Fig.7 shows the comparison between peak stresses obtained by the compression tests and calculated by the established constitutive models. Apparently, the calculated values agree well with the actual values for both holding time. This indicates that these two constitutive models have accurate predictability for the deformation behavior of U720Li alloy.

2.3 Establishment of processing maps

Processing maps are usually used to study the hot workability of superalloys[25]. Based on the dynamic materials model (DMM), the total power (P) can be divided into two parts: the power dissipated by plastic work (G) and the power dissipated by microstructural evolution (J), such as dynamic recovery, DRX and phase transformation. Hence, the P can be expressed as follows[26–27]:

$$P=G+J=\int_0^{\dot{\varepsilon}}\sigma\mathrm{d}\dot{\varepsilon}+\int_0^{\sigma}\dot{\varepsilon}\mathrm{d}\sigma \quad (7)$$

When the strain and deformation temperature are constant, the flow stress can be expressed as $\sigma=K\dot{\varepsilon}^m$, where K is a material constant and m is the strain rate sensitivity. Then, Eq.(7) can be derived as[5]:

$$P=\int_0^{\sigma}\left(\frac{\sigma}{K}\right)^{\frac{1}{m}}\mathrm{d}\sigma+\int_0^{\dot{\varepsilon}}K\dot{\varepsilon}^m\mathrm{d}\dot{\varepsilon}=\frac{\dot{\varepsilon}\sigma m}{m+1}+\frac{\dot{\varepsilon}\sigma}{m+1} \quad (8)$$

It can be seen that the energy dissipated by G and J depends on m, and the m can be denoted by:

$$m=\frac{\mathrm{d}J}{\mathrm{d}G}=\left[\frac{\partial(\ln\sigma)}{\partial(\ln\dot{\varepsilon})}\right]_{\varepsilon,T} \quad (9)$$

Under the given strain and deformation temperature occasions, the J can be described as:

$$J=\int_0^{\sigma}\dot{\varepsilon}\mathrm{d}\sigma=\frac{\dot{\varepsilon}\sigma m}{m+1} \quad (10)$$

However, in the actual hot deformation process, the energy of the specimen cannot be linearly dissipated. Generally, the

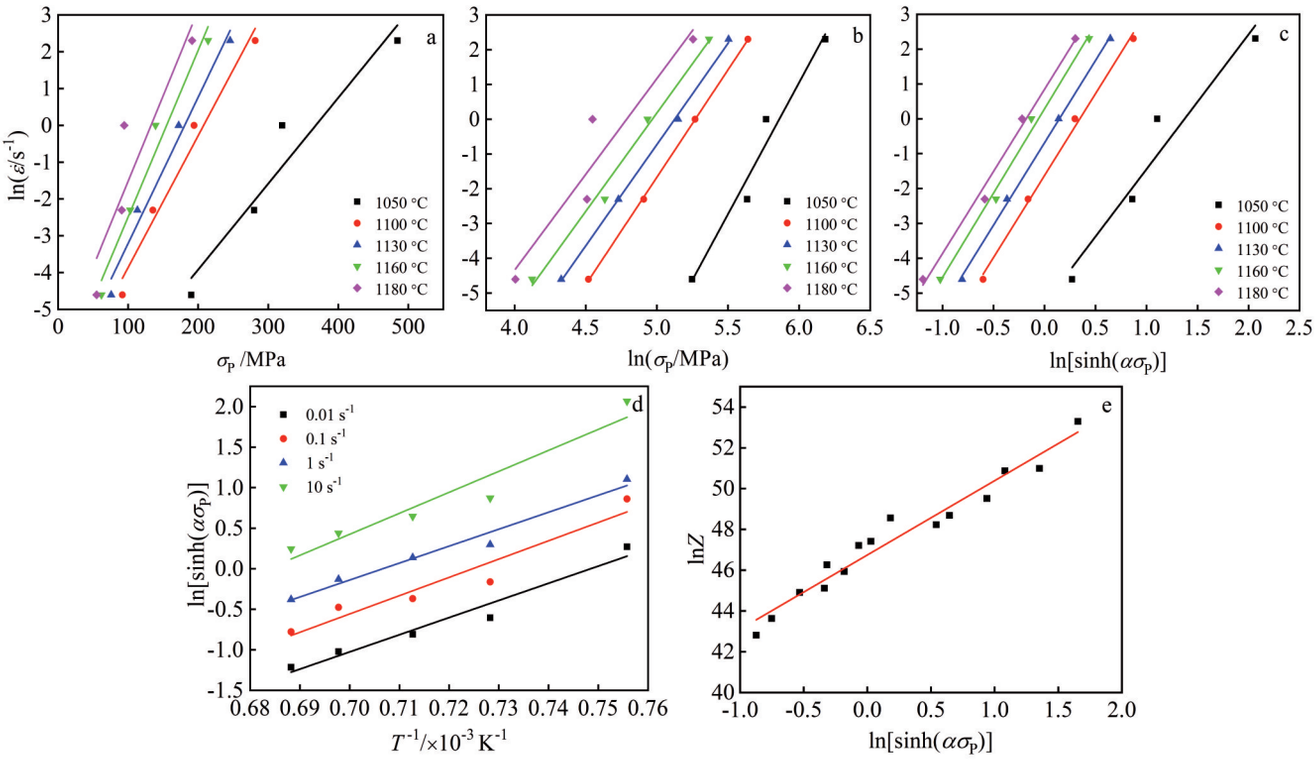

Fig.6 Plots of $\ln\dot{\varepsilon}$-σ_p (a), $\ln\dot{\varepsilon}$-$\ln\sigma_p$ (b), $\ln\dot{\varepsilon}$-$\ln[\sinh(\alpha\sigma_p)]$ (c), $\ln[\sinh(\alpha\sigma_p)]$-$1/T$ (d), and $\ln Z$-$\ln[\sinh(\alpha\sigma_p)]$ (e) for the holding time of 10 min

Table 3 Kinetic parameters of U720Li alloy for the holding time of 10 min

β	n_1	n	α	Q/kJ·mol^{-1}	ln$A$
0.038	6.181	4.569	0.00615	850.996	71.660

power dissipation efficiency (η) is introduced to assess the power dissipation capacity of the specimen, which can be evaluated as[23]:

$$\eta = \frac{J}{J_{max}} = \frac{2m}{(m+1)} \tag{11}$$

The power dissipation maps can be established according to the variation of η. Domains with high η is usually identified as the optimum processing conditions, which needs to be verified by the deformation microstructure. However, the high η does not ensure the optimal hot workability, because the microstructure evolution of superalloys during hot deformation is quite complex. In order to characterize unstable domains accurately, the indicator ξ which represents the material instability is defined as follows[5,28]:

$$\xi(\dot{\varepsilon}) = \frac{\partial \ln\left[m/(m+1)\right]}{\partial \ln \dot{\varepsilon}} + m \leqslant 0 \tag{12}$$

It can be deduced from Eq.(12) that the unstable domains are characterized by the negative value of ξ. Based on the variations of flow instability parameter under all deformation conditions, instability maps can be constructed. By superimposing the instability maps over power dissipation maps, the processing maps will be constructed. The detailed steps to establish the processing map have been described in Ref.[5,29].

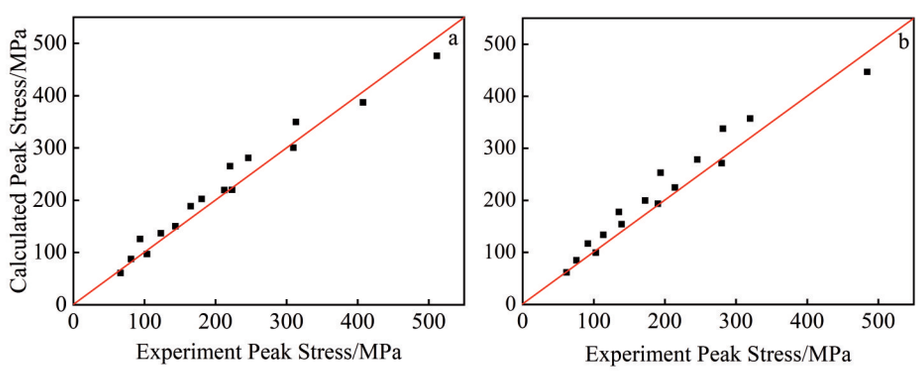

Fig.7 Comparison between peak stresses obtained by the compression tests and calculated by the established constitutive models for the holding time of 5 min (a) and 10 min (b)

2.4 Effect of holding time on processing maps

Processing maps of U720Li alloy are established within the temperature range of 1050–1180 °C and strain rate range of 0.01–10 s^{-1}. The domains with a gray color represent unstable zones and those with a white color denote stable zones.

Fig. 8 shows the processing map for the holding time of 5 min. The processing map contains three domains, and the workability of U720Li alloy in each domain is discussed in combination with microstructure observation. Domain A is the stable zone with high η value as 28% – 41%. The corresponding microstructure proves that obvious DRX occurs and no deformation defects form in Domain A. However, when the strain rate is lower than 0.1 s^{-1}, incomplete DRX structure forms, which will cause an adverse effect on the service performance of the alloy, e. g., vulnerable to crack initiation[30].

Domain B is the unstable zone with low η value of 15%–25% in the temperature range of 1050–1090 °C and strain rate range of 0.1–10 s^{-1}. Mixed grain structures with coarse grains distributed in chain shapes form in this domain, which will deteriorate mechanical properties of the alloy[31]. Domain C is also the unstable zone with η value of 17% – 28% and negative ξ value, which exists in the temperature range of 1110–1145 °C and strain rate range of 1–10 s^{-1}. Mixed grain structures also form in Domain C. It is widely accepted that the adiabatic heating usually occurs during hot deformation at high strain rates owing to the insufficient deformation time[9]. The occurrence of adiabatic heating leads to rapid grain coarsening in local regions, and hence the mixed grain structures form. Consequently, the optimum processing conditions for the holding time of 5 min are determined to be 1090–1110 °C/1–10 s^{-1} and 1146–1180 °C/1–10 s^{-1}.

Fig. 9 shows the processing map for the holding time of 10 min, which contains four domains. Domain A is the stable zone with high η value of 28%–39%, indicating that the main deformation mechanism is DRX. According to the corresponding microstructure observation, obvious DRX takes place and no deformation defects form in this domain. Also, incomplete DRX occurs when the strain rate is lower than 0.1 s^{-1}.

Domain B is the unstable zone in the temperature range of 1050 – 1073 °C and strain rate range of 0.01 – 0.1 s^{-1}. The corresponding microstructure suggests that the main instability mechanism in Domain B is characterized by local plastic flow, and the flow localization band is approximately 35° away from the compression axis direction. The local plastic flow is easy to occur at low deformation temperatures[32]. Domain C is also the unstable zone with low η value of 11%–28% in the temperature range of 1091–1153 °C and strain rate range of 0.5 – 10 s^{-1}. Based on the corresponding microstructure, the instability mechanism in Domain C is characterized by the adiabatic shear band which is caused by severe plastic deformation localization. In such unstable zone, the shear deformation is very concentrated and cracking is easy to occur. Moreover, the formation of flow localization and adiabatic shear band can induce poor mechanical properties of the final products[33].

Domain D with high η value (the maximum value is about

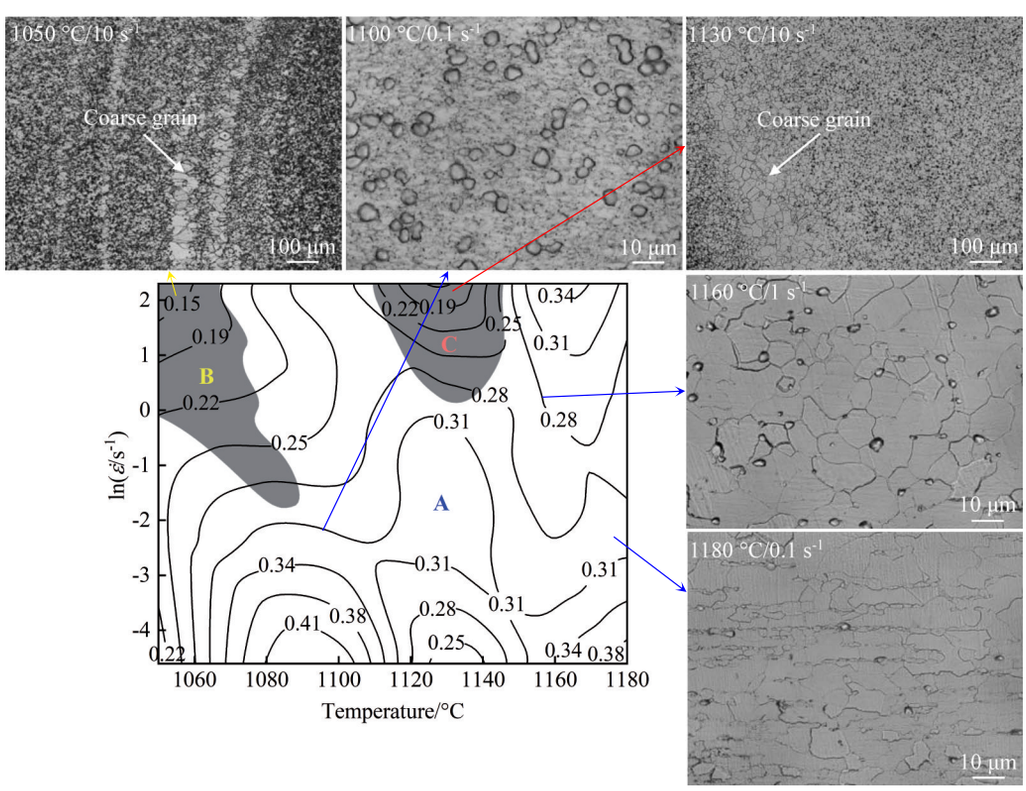

Fig.8 Processing map for the holding time of 5 min with microstructure validation in different domains

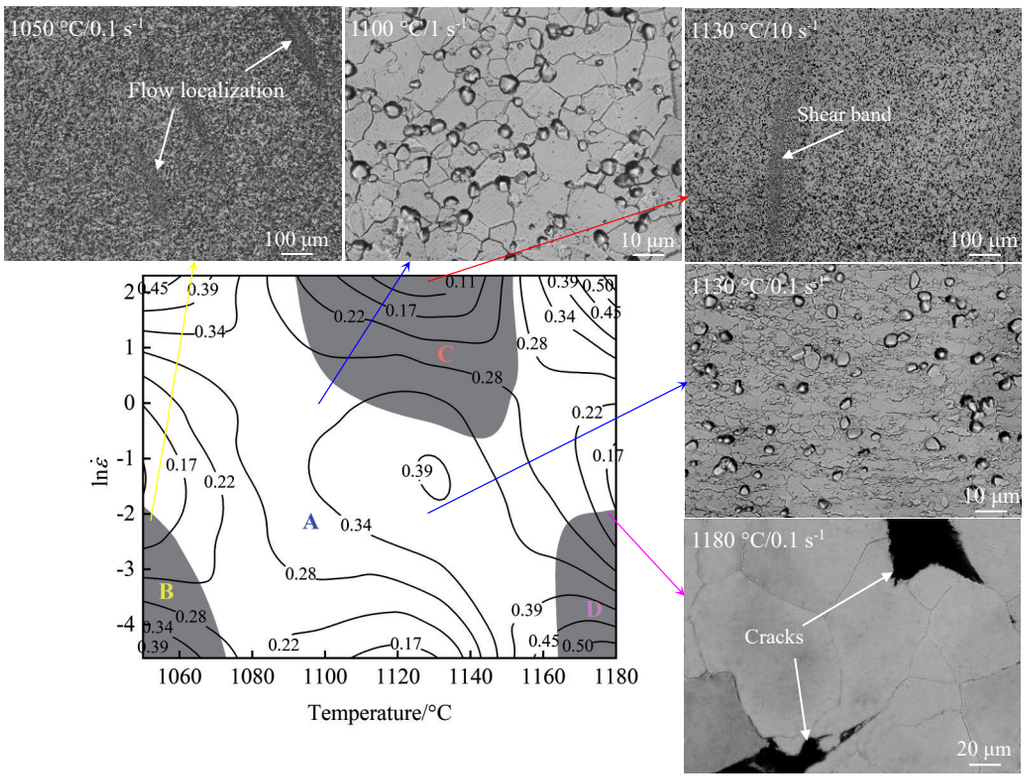

Fig.9 Processing map for the holding time of 10 min with microstructure validation in different domains

50%) and negative ξ value exists in temperature range of 1164–1180 °C and strain rate range of 0.01–0.1 s^{-1}. The high η value indicates that this domain should be a stable zone. However, the specimens deformed at 1180 °C crack obviously and wedge-shaped cracks appear at triple junctions of grain boundaries. Thus, Domain D is actually a severe instability zone. Several studies have reported that the wedge cracking usually occurs at high temperatures[34–35]. Generally, the power dissipation efficiency by cracking is high (close to that for superplasticity), because the energy conversion efficiency into surface energy is very high[36].

Apparently, the instability mechanism for the holding time of 10 min is quite different from that for the holding time of 5 min. The optimum processing conditions for the holding time of 10 min are determined to be 1080–1090 °C/1–10 s^{-1} and 1153–1160 °C/1–10 s^{-1}. Compared with the holding time of 5 min, the safe processing window for the holding time of 10 min is obviously narrower. The prolongation of holding time increases the degree of γ' dissolution, especially at high temperatures, which weakens its pinning effect on grain boundaries. Then, the adhesion of grain boundaries is weakened and more significant grain coarsening occurs before deformation, which deteriorates the hot workability and makes it more prone to intergranular cracking. Based on Yu et al's research[8], it is worth noting that the optimum processing conditions for U720Li alloy should be 1090–1130 °C/0.08–0.5 s^{-1} plus 0.005–0.008 s^{-1}, and 1040–1085 °C/0.005–0.06 s^{-1}. This is not consistent with the findings in this study, which is mainly because their research temperature range (1040–1130 °C) and strain rate range (0.005–0.5 s^{-1}) are quite different from those in this study, and the holding time before deformation was not introduced in their study.

2.5 Microstructure evolution at various deformation conditions

The characteristic of flow stress curves indicates that the DRX should occur under all deformation conditions[10,37]. Fig. 10 shows the deformation microstructures of U720Li alloy with the holding time of 5 min. When the deformation temperature is lower than of 1100 °C, a large number of γ' particles remain and the grain structure is relatively fine. For the strain rate of 0.01 s^{-1}, some new grains form around the γ' particles. With the increase in strain rate to 0.1 s^{-1}, lots of finer new grains form around the γ' particles. With further increasing the strain rate to 1 s^{-1} or above, the matrix is fully composed of new grains. But the initial grain boundaries are not obviously bowed.

When the deformation temperature is higher than 1130 °C, the amount and size of residual γ' decrease markedly with increasing the temperature. For the strain rate lower than 0.1 s^{-1}, obvious bowing occurs at initial grain boundaries and fine new grains form along the initial grain boundaries, forming the "necklace structure". When the strain rate is increased to 1 s^{-1} or above, the matrix is also full of new grains, which indicates that the alloy undergoes complete DRX.

Fig. 11 shows the deformation microstructures for the holding time of 10 min. When the deformation temperature is below 1160 °C, the influence of temperature and strain rate on

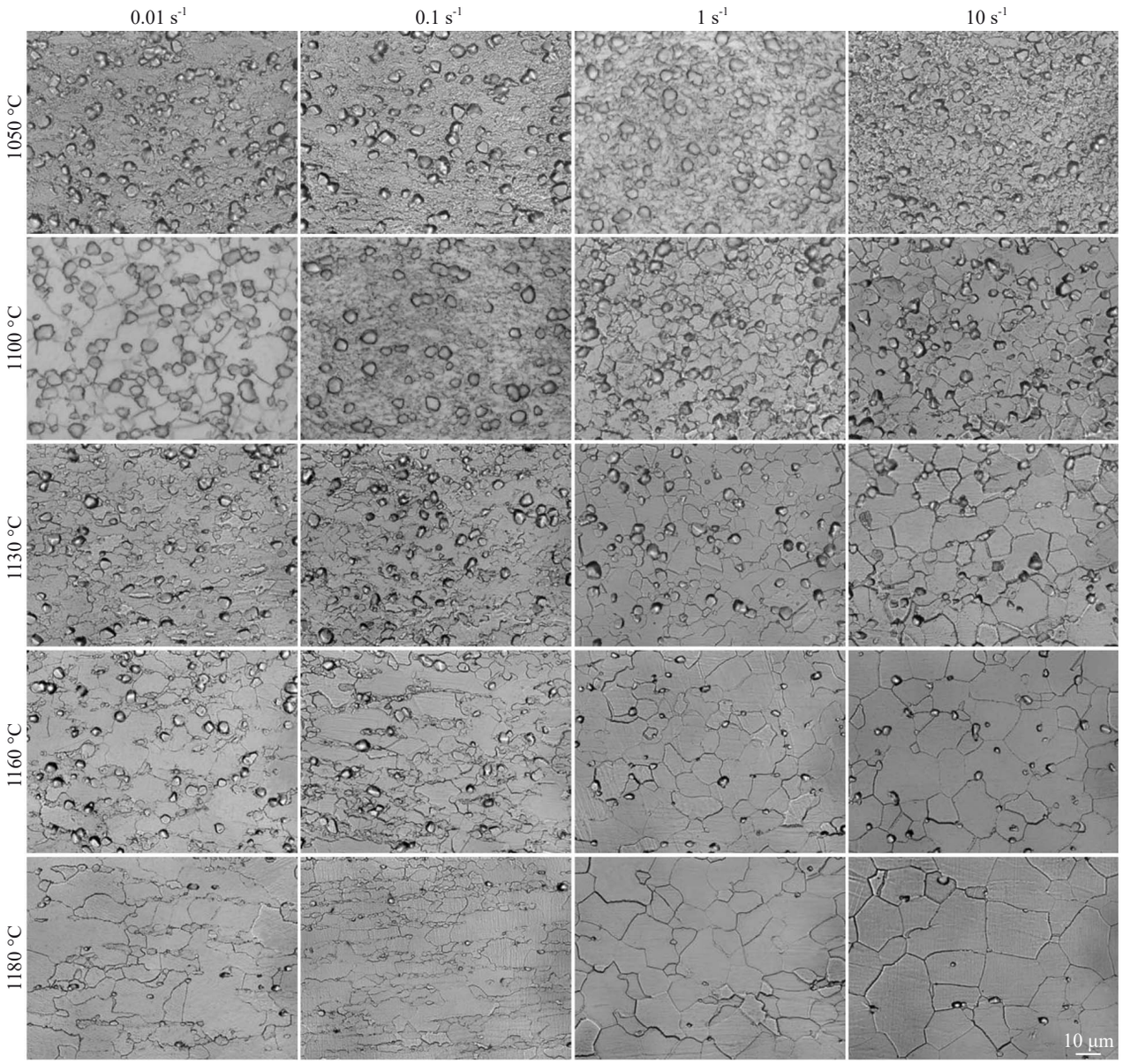

Fig.10 Microstructures of U720Li alloy deformed at different temperatures and strain rates with a holding time of 5 min

the DRX behavior is basically consistent with that for the holding time of 5 min. However, when the deformation temperature reaches 1180 °C, the extension of holding time to 10 min leads to the complete dissolution of γ', which causes the disappearance of γ' pinning effect on grain boundaries. Hence, the migration of grain boundaries is promoted, and then the grain structure becomes much coarser. But when the strain rate is further increased to 10 s^{-1}, the DRX grain size becomes much smaller. This may be because the much higher strain rate enhances the dislocation pile-up and increases the stored energy, thus facilitating the DRX process[38].

For each holding time, when the deformation temperature is below 1100 ° C, the γ' particles can effectively hinder the movement of dislocations, forming high density dislocation substructures and subgrain boundaries within initial grains. As the deformation proceeds, the subgrains continuously absorb dislocations, leading to the occurrence of DRX ultimately, which is the PI-CDRX[11]. When the deformation temperature is increased to above 1130 ° C, initial grain boundaries bow obviously and the "necklace structure" forms, which indicates that the main DRX mechanism becomes DDRX[21]. Obviously, the DRX mechanism at low temperatures is different from that in Ref. [11 – 12], but at high temperatures it is similar to that in Ref. [12]. The change in DRX mechanism with deformation temperature is mainly related to the amount of residual γ' and its interaction with dislocations. The lower γ' fraction is beneficial to grain boundary migration which promotes the DRX nucleation through the bulging of initial grain boundaries.

Fig. 12 shows the effect of deformation condition on the DRX grain size. In the absence of cracking, the DRX grain size first decreases as the strain rate increases to 0.1 s^{-1}, and

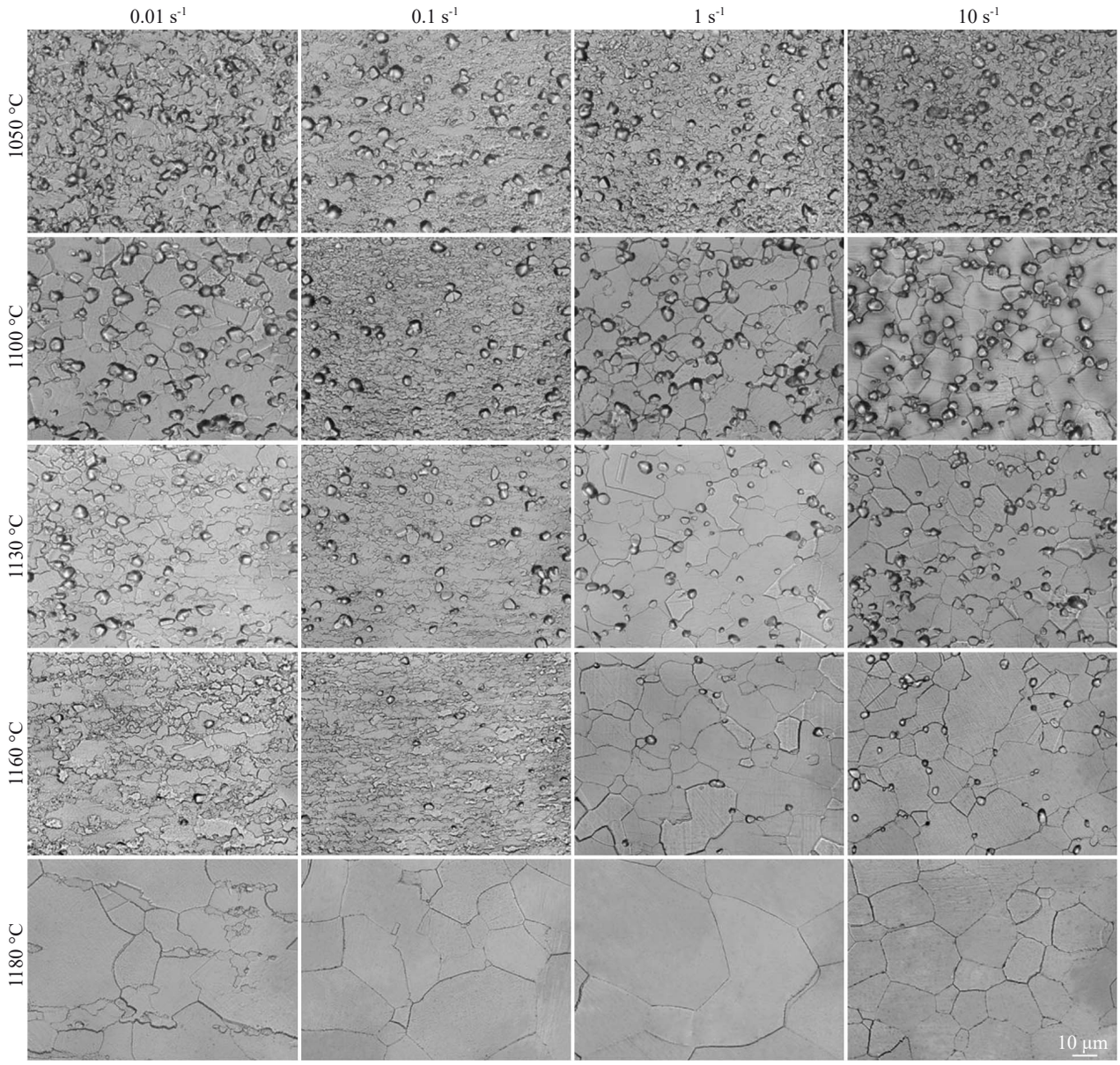

Fig.11 Microstructures of U720Li alloy deformed at different temperatures and strain rates with a holding time of 10 min

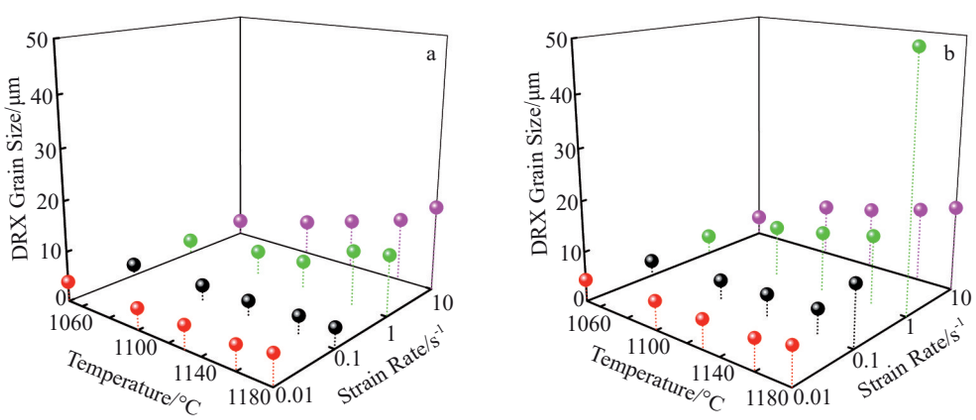

Fig.12 Effect of deformation condition on the DRX grain size for the holding time of 5 min (a) and 10 min (b)

then increases as the strain rate increases to above 1 s^{-1}. The main reason is that as the strain rate increases to 0.1 s^{-1}, the stored energy increases obviously, which promotes the nucleation of DRX. But as the strain rate further increases to above

1 s^{-1}, significant adiabatic temperature rise occurs, which markedly promotes the growth of DRX grains. Besides, the DRX grain size increases gradually as the deformation temperature increases, and the DRX grain size for the holding time of 10 min is obviously greater than that for the holding time of 5 min. This is mainly due to the higher γ' dissolution degree at higher holding temperatures with longer holding durations.

3 Conclusions

1) The flow stress increases with rising of strain rate, while decreases with the increase in deformation temperature and holding time. The Arrhenius-type constitutive models for two holding time are established as follows: for the holding time of 5 min, $\dot{\varepsilon} = 2.106 \times 10^{36}\left[\sinh\left(0.00608\sigma_p\right)\right]^{4.618} \exp\left(-\frac{992006}{RT}\right)$; for the holding time of 10 min, $\dot{\varepsilon} = 1.323 \times 10^{31}\left[\sinh\left(0.00615\sigma_p\right)\right]^{4.569} \exp\left(-\frac{850996}{RT}\right)$.

2) Processing maps for the holding time of 5 and 10 min are constructed. The optimal hot working conditions for the holding time of 5 min are determined to be 1090–1110 °C/1–10 s^{-1} and 1146–1180 °C/1–10 s^{-1}, while those for holding time of 10 min are 1080–1090 °C/1–10 s^{-1} and 1153–1160 °C/1–10 s^{-1}. The safe processing window will be narrowed due to the overlong holding time.

3) In the absence of cracking, as the strain rate increases from 0.01 s^{-1} to 0.1 s^{-1}, the DRX grain size decreases markedly. But when the strain rate further increases from 0.1 s^{-1} to 10 s^{-1}, the DRX grain size increases significantly. Besides, the DRX grain size increases gradually with the increase in deformation temperature and holding time.

4) The DRX mechanism is mainly PI-CDRX when the deformation temperature is lower than 1100 °C, but it changes to DDRX as the deformation temperature is increased to above 1130 °C.

References

1 Bi Z, Qu J, Du J *et al. Procedia Engineering*[J], 2012, 27: 923

2 Keefe P W, Mancuso S O, Maurer G E. *Superalloys 1992*[C]. Warrendale: TMS, 1992: 487

3 Wang T, Li Z, Fu S H *et al. Advanced Materials Research*[J], 2013, 709: 143

4 Yu Q Y, Yao Z H, Dong J X. *Materials Characterization*[J], 2015, 107: 398

5 Wen D X, Lin Y C, Li H B *et al. Materials Science & Engineering A*[J], 2014, 591: 183

6 Qu J L, Bi Z N, Du J H *et al. Journal of Iron and Steel Research, International*[J], 2011, 18: 59

7 Li Z, Fu S H, Wang T *et al. Materials Science Forum*[J], 2013, 747: 588

8 Yu Q Y, Yao Z H, Dong J X. *International Journal of Minerals, Metallurgy and Materials*[J], 2016, 23: 83

9 Wan Z, Hu L, Sun Y *et al. Journal of Alloys and Compounds*[J], 2018, 769: 367

10 Liu F, Chen J, Dong J *et al. Materials Science & Engineering A*[J], 2016, 651: 102

11 Li X X, Jiang Z H, Wan Z P *et al. Journal of Materials Engineering & Performance*[J], 2020, 29: 6343

12 Wan Zhipeng. *Hot Deformation Behavior and Microstructure & Properties Control of Ni-based Alloy GH4720Li*[D]. Harbin: Harbin Institute of Technology, 2019 (in Chinese)

13 Zhao Guangdi, Zang Ximin, Zhao Zhuo. *Rare Metal Materials and Engineering*[J], 2020, 49(11): 3809

14 Shi Z X, Yan X F, Duan C H *et al. Journal of Iron and Steel Research, International*[J], 2017, 24: 625

15 Monajati H, Taheri A, Jahazi M *et al. Metallurgical and Materials Transactions A*[J], 2005, 36: 895

16 Ning Y Q, Wang T, Fu M W *et al. Materials Science & Engineering A*[J], 2015, 642: 187

17 Zhou Ge, Ding Hua, Han Yinben *et al. Rare Metal Materials and Engineering*[J], 2014, 43(1): 72 (in Chinese)

18 Fan H, Jiang H, Dong J *et al. Journal of Materials Processing Technology*[J], 2019, 269: 52

19 Somani M, Muraleedharan K, Prasad Y *et al. Materials Science & Engineering A*[J], 1998, 245: 88

20 Guimaraes A A, Jonas J J. *Metallurgical and Materials Transactions A*[J], 1981, 12: 1655

21 Zhao G, Zang X, Jing Y *et al. Materials Science & Engineering A*[J], 2021, 815: 141293

22 Zheng R, Gong W, Du J *et al. Acta Materialia*[J], 2022, 238: 118243

23 Sajjadi S A, Chaichi A, Ezatpour H R *et al. Journal of Materials Engineering & Performance*[J], 2016, 25: 1269

24 Ma Tengfei, Du Gang, Qi Rui *et al*. *Rare Metal Materials and Engineering*[J], 2020, 49(1): 201 (in Chinese)

25 Prasad Y V R K, Gegel H L, Doraivelu S M *et al. Metallurgical Transactions A*[J], 1984, 15: 1883

26 Babu K A, Mandal S, Kumar A *et al. Materials Science & Engineering A*[J], 2016, 664: 177

27 Jiang He, Wang Fa, Li Xin *et al*. *Rare Metal Materials and Engineering*[J], 2021, 50(1): 349 (in Chinese)

28 Zhou Ge, Li Jianlin, Men Yue *et al*. *Rare Metal Materials and Engineering*[J], 2021, 50(4): 1318 (in Chinese)

29 Wen D X, Lin Y C, Chen J *et al. Materials Science & Engineering A*[J], 2015, 620: 319

30 Zhang B, Wang Z, Yu H *et al*. *Journal of Alloys and Compounds*[J], 2022, 900: 163515

31 Konkova T, Rahimi S, Mironov S *et al*. *Materials Characterization*[J], 2018, 139: 437

32 Yang Y T, Luo R, Cheng X N *et al. Chinese Journal of Materials Research*[J], 2019, 33: 232

33 Kartika I, Li Y, Matsumoto H *et al*. *Materials Transactions*[J], 2009, 50(9): 2277

34 Raj R. *Metallurgical Transactions A*[J], 1981, 12: 1089
35 Ashby M F. *Acta Metallurgica*[J], 1972, 20: 887
36 Patnamsetty M, Somani M C, Ghosh S *et al. Materials Science & Engineering A*[J], 2020, 793: 139840
37 Chen J, Dong J, Zhang M *et al. Materials Science & Engineering A*[J], 2016, 673: 122
38 Jiang H, Dong J, Zhang M *et al. Metallurgical and Materials Transactions A*[J], 2016, 47: 5071

保温时间对难变形高温合金U720Li热变形行为的影响

臧喜民[1]，赵广迪[2]，武金江[2]，姜昊源[2]，姚晓雨[3]
(1. 沈阳工业大学 材料科学与工程学院，辽宁 沈阳 110870)
(2. 辽宁科技大学 材料与冶金学院，辽宁 鞍山 114051)
(3. 中国科学院 金属研究所，辽宁 沈阳 110016)

摘 要：为了改善难变形高温合金U720Li的热加工性能，研究了变形前保温时间（5和10 min）对该合金的热变形行为的影响。结果表明，流动应力随应变速率的提高而增大，但随变形温度和保温时间的增加而减小。依据所建立的Arrhenius本构模型计算的峰值应力与实验值吻合良好，说明该模型可准确预测U720Li合金热变形行为。保温时间为5和10 min的热变形激活能分别为992.006和850.996 kJ·mol^{-1}。建立了U720Li合金在这2种保温时间下的热加工图。通过分析热加工图各区域对应的变形组织，明确了保温5 min的最佳热加工条件为1090~1110 ℃/1~10 s^{-1}和1146~1180 ℃/1~10 s^{-1}，而保温10 min的最佳热加工条件为1080~1090 ℃/1~10 s^{-1}和1153~1160 ℃/1~10 s^{-1}。可见适当缩短变形前保温时间可扩大该合金的安全加工窗口。在未发生开裂的情况下，动态再结晶（DRX）晶粒随变形温度和保温时间的增加而逐渐增大，但随应变速率的增加先减小后增大。当变形温度低于1100 ℃，主要DRX机制为颗粒诱导连续DRX。当变形温度高于1130 ℃，主要DRX机制转变为不连续DRX。

关键词：难变形高温合金；热变形行为；热加工图；动态再结晶

作者简介：臧喜民，男，1978年生，博士，教授，沈阳工业大学材料科学与工程学院，辽宁 沈阳 110870，E-mail：zangxm@sut.edu.cn